Tunable ligand discrimination via kinetic sorting

Purushottam Dixit,[1,2,a)] Andrew Goetz,[1] and Ralitsa Madsen[3]
[1)] *Department of Biomedical Engineering, Yale University, New Haven, CT*
[2)] *Systems Biology Institute, Yale West Campus, West Haven, CT, 06516*
[3)] *MRC Protein Phosphorylation and Ubiquitylation Unit, University of Dundee, Dundee, DD1 5EH*

Abstract. *Kinetic proofreading* is a class of non-equilibrium mechanisms that allow biochemical sensing networks to discriminate between cognate and non-cognate ligands. Proofreading is typically invoked in the context of error correction and therefore is often inflexible in its discrimination in favor of the cognate ligand. This discrimination is achieved when a multi-step and energy consuming reaction pathway is irreversibly restarted with a rate proportional to the thermodynamic stability of the ligand-bound complex. Here, we present a novel non-equilibrium and tunable *kinetic sorting* mechanism that allows signaling networks to modulate ligand discrimination in direction as well as in magnitude. In our model, the 'restart cycle' associated with traditional proofreading is coupled with a topologically distinct and ligand-identity independent cycle, e.g., through receptor degradation or activity-induced desensitization. The signaling network can *kinetically sort* the non-equilibrium flux of receptors bound to one of the ligands towards degradation/desensitization and the other through the restart cycle. This preferential diversion of the non-equilibrium flux allows the network to switch its ligand discrimination by altering biochemical processes that are not specific to the identity of the bound ligand, thereby allowing cells to respond to ligands in a context-specific manner. Our model recapitulates several observations related to paradoxical ligand discrimination by the Epidermal Growth Factor pathway. Given the ubiquity of receptor degradation, activity-induced desensitization, and other similar cycles in cellular signaling networks, tunable ligand discrimination using *kinetic sorting* is likely to be broadly applicable.

I. INTRODUCTION

Cellular signaling networks often interact with myriads of extracellular stimuli and respond in a context-specific manner[1,2]. Understanding the underlying biochemistry and computational principles that allow signaling networks to differentiate between input stimuli and transduce appropriate downstream responses is of great importance, given that the inability to decode environmental stimuli is responsible[3], at least in part, for several diseases including diabetes and cancers.

In 1970s, John Hopfield[4] and Jacques Ninio[5] proposed non-equilibrium mechanisms to explain how enzymes such as ribosomes discriminate between cognate and non-cognate ligands beyond pure thermodynamic preference. Similar mechanisms were later proposed in other contexts such as protein folding[6], DNA disentanglement[7], DNA replication[8], mRNA surveillance[9], cellular signaling[10,11], as well as in synthetic biology[12], establishing the so-called concept of *kinetic proofreading*[13–16] as a broadly applicable mechanism to achieve extra-thermodynamic discrimination in biochemical networks.

A common theme across kinetic proofreading mechanisms is that a series of non-equilibrium and irreversible transformations create high-energy intermediates which frequently restart the signaling process at the expense of free energy[15]. The *extra-thermodynamic* boost in ligand discrimination is related to the difference in restart rates of non-cognate and cognate intermediates. While most kinetic proofreading studies focus on energetically futile cycles of chemical modifications (e.g. , phosphorylation/dephosphorylation), recent work has also highlighted novel proofreading mechanisms, e.g. , through restarting diffusion in physical space (instead of the chemical state space) towards a target state[17].

Typical proofreading mechanisms are invoked in situations where cognate and the non-cognate inputs are present simultaneously and the task of the network is to minimize the error (e.g. , signaling from the non-cognate input). Therefore, proofreading mechanisms have largely been explored in the context of enhancing ligand discrimination in favor of the cognate ligand. Notably, previous works have discussed the possibility of *anti-proofreading*[18] wherein networks can prefer weakly binding ligands over the strong binding ligand. However, as we will show below, the specific pathways invoked in our models do not adhere to the essential prescription of the *anti-proofreading model*[18].

Cellular signaling networks are often faced with a different problem to that of simple proofreading. These networks typically respond to more than one ligand, often in a context-specific manner. An example is families of receptor tyrosine kinases (RTKs) such as the epidermal growth factor (EGF) receptor (EGFR). EGFRs interact with several ligands including high-affinity ligands such as EGF and transforming growth factor β (TGFβ) and low affinity ligands such as epiregulin (EREG) and epigen (EPGN)[19]. Notably, different ligands lead to qualitative and quantitatively different EGFR activity profiles and consequently downstream cellular phenotypes. Therefore, ligands that interact with cellular signaling networks often cannot be classified as cognate versus non-cognate.

[a)] email:purushottam.dixit@yale.edu

Instead, it is crucial to understand how cells modulate non-equilibrium processes to make signaling circuits recognize and respond differently to different cognate ligands.

Notably, in addition to non-equilibrium restart cycles in traditional proofreading that may arise from ligand dissociation or receptor de-oligomerization, many cellular signaling networks are endowed with additional topologically distinct cycles. These include synthesis and preferential degradation of ligand-activated receptors commonly seen for RTKs such as EGFRs[20] and G protein coupled receptors (GPCRs)[21], and activity-induced desensitization and reactivation which are seen for GPCRs[22] and ligand-gated ion channels[23]. These cycles are likely to consume a significantly higher amount of energy compared to the restart cycle. For example, in MCF10A cells, there are $\sim 10^5$ EGFRs on the cell surface (receptor length: 1210 amino acids)[24] that are constantly synthesized and degraded. The estimated steady state rate of receptor synthesis is ~ 15 receptors per second[25], corresponding to energy consumption of $\approx 8 \times 10^4$ ATP/sec (assuming ~ 4.5 ATP molecules per peptide bond)[26]. In contrast, the dephosphorylation time scale of EGF receptors is ~ 15 seconds[27]. Moreover, typically only $5 - 10\%$ of all receptors are phosphorylated[24,28]. The corresponding ATP consumption due to energetically futile dephosphorylation cycles is $0.1 \times 10^5/15 \sim 6 \times 10^2$ATP/sec, a number that is around two orders of magnitudes lower compared to the energy consumed in receptor synthesis and degradation.

These cycles often operate to subdue the ultimate activated species in the multi-step activation process (e.g. preferential degradation of the ultimate phosphorylated state and induced desensitization of active GPCRs and ion channels). Given that strong-binding and slow time-scale ligands are likely to frequent the ultimate chemical state more often compared to the weak-binding and fast time-scale ligands, these additional loops may give signaling networks extra freedom to modulate their encoding of external ligands. While these cycles have been hypothesized to control ligand discrimination[29,30], their quantitative role remains unknown.

To understand how these topologically distinct cycles interact with the traditional proofreading mechanism, we present a simple mechanistic model of a ligand/receptor signaling network. In the model, ligand-bound receptors undergo multiple steps of phosphorylation before they are either preferentially degraded, or desensitized followed by a slow resensitization step. The model also has the restart cycle associated with traditional proofreading wherein receptors can dissociate from the ligand at any stage to restart the signaling process. Using this model, we propose a new discrimination mechanism of *kinetic sorting*. Here, depending on rate parameters, the signaling network can *kinetically sort* the non-equilibrium flux of receptors bound to one of the ligands towards degradation/desensitization. This preferential diversion of the non-equilibrium flux allows the network to achieve differential signal encoding in response to different ligands.

Given the ubiquity of non-equilibrium cycles of receptor degradation, activity-induced desensitization and resensitization, and other such cycles in cellular signaling networks, tunable ligand discrimination using *kinetic sorting* is likely to be broadly applicable and central to their remarkable computing abilities.

II. RESULTS

A recent paradoxical observation about ligand discrimination by the EGFR pathway motivates our work[29]. It was shown that the steady state EGFR phosphorylation response was significantly higher for the weak-binding ligand Epigen compared to the strong-binding ligand EGF, even when cells were exposed to saturating ligand levels. This discrimination in favor of the weak-binding ligand is in the opposite direction to what is dictated by traditional kinetic proofreading. We therefore seek to identify simplified signaling networks that qualitatively mimic this behavior.

To keep our analysis simple, our model makes several simplifying assumptions. We note that in many receptor families including, RTKs such as EGFRs and T cell receptors, ligand binding leads to receptor oligomerizationwhich in turn leads to receptor activation[1]. In the model, we assume that monomeric ligand-bound receptors are sufficient for receptor activation. Moreover, as is typically done in proofreading models[15], we assume that the binding free energy difference between two ligands arises entirely due to differences in dissociation rates. Effectively, these approximations imply that the ligand dissociation rate used in our model is the rate limiting step between receptor de-oligomerization and ligand dissociation. Moreover, the difference in dissociation rates encodes the difference in binding strengths. Therefore, a weak-binding and fast-dissociating ligand in our model can be considered equivalent to a ligand that causes fast undimerization of the receptors and vice versa for strong-binding and slow-dissociating ligands. Another assumption is the lack of dephosphorylation reactions[27]. Notably, as we show in supplementary materials, inclusion of dephosphorylation does not change the qualitative behavior of the model. Finally, the model neglects endosomal compartments and receptor recycling[31]. As shown in supplementary materials, this too does not change the qualitative behavior of the model.

A. Traditional proofreading favors slow-dissociating ligands.

To illustrate the role of coupling between non-equilibrium cycles, we start with a model of receptor-based proofreading, similar to the one proposed by McKeithan to explain how T cell receptors (TCRs) avoid activation when interacting with non-cognate lig-

ands[10]. Notably, several topological features of the model (e.g. multi-step activation and fast phosphorylation/dephosphorylation) are shared between TCRs and RTKs. A schematic of the model is shown in Fig. 1. In the model, receptors bind to ligands and are subsequently phosphorylated in a series of reactions. Similar to McKeithan's model, the ultimate phosphorylated receptor P_N is assumed to be the signaling competent species. Proofreading arises from the fact that intermediate phosphorylated states $P_M, M \in [1, N]$ can lose the bound ligand (and phosphorylation(s)) and revert back to the ligand-free unphosphorylated receptor R. We evaluate the signaling output when the network is separately exposed to two ligands L_1 and L_2. For simplicity, we assume that all reactions rates are identical between the two ligands except for the ligand dissociation rate. Without loss of generality, we assume that ligand 2 dissociates faster compared to ligand 1.

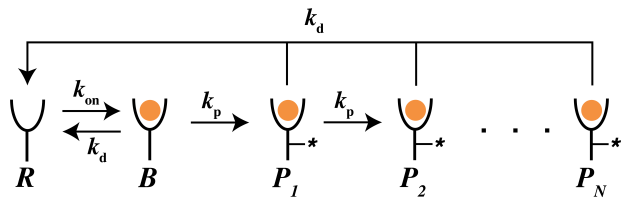

FIG. 1. **Reaction scheme of a simple RTK model without receptor degradation**. Chemical species and rate constants are shown in the figure. R denote ligand-free receptors, B denote ligand-bound inactive receptors, and $P_m, m \in [1, N]$ are phosphorylated receptors. The ultimate phosphorylated species P_N is assumed to be signaling competent. Elsewhere in the text, the rate constants specific to ligands 1 and 2 are denoted by an additional subscript (not shown in this figure).

The discrimination between two ligands arising from thermodynamics of ligand binding is given by

$$\varepsilon_{\text{th}} = \frac{u_1(1+u_2)}{u_2(1+u_1)} \tag{1}$$

where $u_1 = L_1/k_{D1}$ and $u_2 = L_2/k_{D2}$ are dimensionless concentrations and $k_{D1} = k_{d,1}/k_{on,1}$ and $k_{D2} = k_{d,2}/k_{on,2}$ are equilibrium dissociation constants for the two ligands respectively. The thermodynamic discrimination ratio accounts for both the entropic contribution related to ligand concentration and the energetic contribution related to the equilibrium dissociation constant. To identify the extra-thermodynamic factors governing ligand discrimination, going forward, we set $u_1 = u_2 = u$ to equalize the thermodynamic contribution to ligand discrimination. Moreover, to recapitulate the observed discrimination in the EGFR pathway at saturating ligand concentrations[29], we assume $u \gg 1$. At steady state, for a network with N phosphorylation states, we define discrimination success ratio $\varepsilon_N = P_{N,1}/P_{N,2}$ as the ratio of concentrations of active receptors species for the two ligands. We have (see supplementary materials)

$$\varepsilon_N = P_{N,1}/P_{N,2} = \left(\frac{\delta+\omega}{1+\omega}\right)^N \tag{2}$$

where $\delta = k_{d,2}/k_{d,1}$ is the ratio of dissociation constants for the two ligands, $\omega = k_p/k_{d,1}$ is the dimensionless phosphorylation rate. Notably, $\delta > 1 \Rightarrow \varepsilon_N > 1$: non-equilibrium thermodynamics can only enhance the discrimination ratio to favor the slow-dissociating ligand over the fast-dissociating ligand.

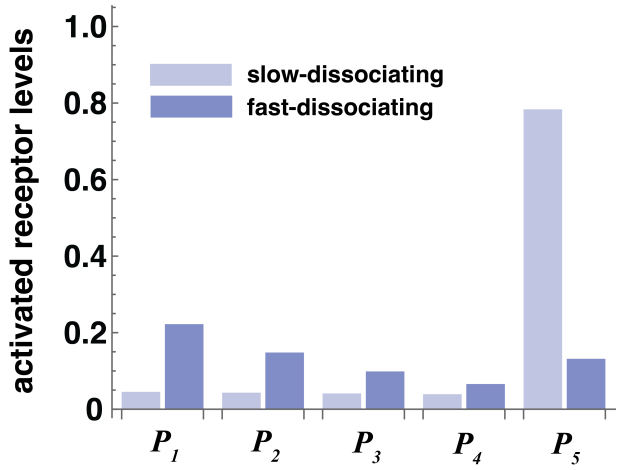

FIG. 2. **Profile of activated receptor concentrations in a multi-step phosphorylation process.** We have used $\omega = 20$ and $\delta = 10$ (see main text for definitions).

Can this discrimination be reversed in favor of the fast-dissociating (low-affinity) ligand? The concentration profile of activated receptors provides a clue. The normalized concentration of the activated receptors in a $N-$step phophorylation chain is given by (see supplementary materials)

$$P_n = \frac{\delta\omega^n}{(\delta+\omega)^{n+1}} \;\forall\; n \in [1, N-1] \tag{3}$$

$$\text{and } P_N = \frac{\omega^N}{(\delta+\omega)^N}. \tag{4}$$

These concentration profiles are plotted in Fig. 2 for the slow-dissociating ($\delta = 1$) and the fast-dissociating ligand ($\delta > 1$). We have used $\omega = 20$ and $\delta = 10$ (derived from Lyashenko et al. [25] and Hu et al.[32]).

When $\omega > \delta > 1$, the ultimate phosphorylation state is significantly more populated in the presence of the slow-dissociating (high-affinity) ligand due to the fact that only the slow-dissociating ligand can reach that ultimate state. Therefore, biochemical processes that selectively target the ultimate state can potentially reverse the direction of discrimination towards the fast-dissociating ligand.

Two mechanisms, amongst potentially many others, that target the final phosphorylated state are typical to

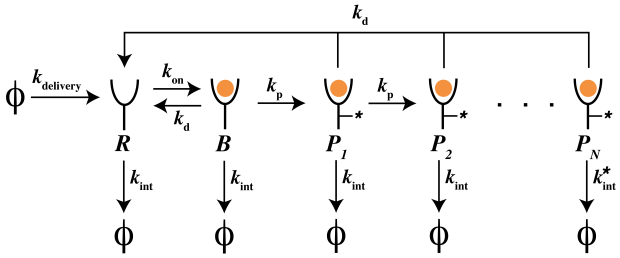

FIG. 3. **Reaction scheme of a simple RTK model with receptor degradation**. Chemical species and rate processes are shown in the figure. R denote ligand-free receptors, B denote ligand-bound inactive receptors, and $P_m, m \in [1, N]$ are phosphorylated receptors. All phosphorylated species are assumed to be signaling competent. Inactive receptors are delivered to the cell surface at a constant rate and all receptors are internalized and degraded. The degradation rate k^*_{int} of the ultimate state P_N is assumed to be higher compared to all other states, irrespective of the bound ligand. The rate constants specific to ligands 1 and 2 are denoted by an additional subscript (not shown in figure).

many cellular signaling networks. For example, a key feature of many RTK and GPCR signaling pathways is preferential degradation of activated receptors[20,21]. Here, once bound to the ligand, receptors quickly dimerize and autophosphorylate to become active. Active receptors recieve multiple further phosphorylations that eventually mark them for degradation. Another mechanism is observed in GPCRsand ligand gated ion channels. Here, the receptors (or channels) become inactivated immediately following ligand-induced desensitization[22,23]. The desensitized receptors/channels cannot participate in signaling and slowly recover back to the ligand-free state. Below, we describe in detail how degradation affects ligand-specific receptor activation. Similar results for activity-induced desensitization are briefly presented later in the manuscript.

To investigate the effect of preferential degradation of activated receptors, we modify the traditional proofreading model (Fig. 3). In this model, ligand-free receptors are constantly delivered to the cell surface at a rate k_{delivery} and internalzied and degraded at a constant rate k_{int}. After ligand-binding, receptors undergo a series of phosphorylation events. A key feature of our model is that fully phosphorylated receptors undergo degradation at a higher $\beta = k^*_{\text{int}}/k_{\text{int}} > 1$ irrespective of the identity of the bound ligand. All phosphorylated receptors are assumed to be signaling competent and are included in the quantification of signaling network output. Finally, similar to traditional proofreading models, phosphorylated receptors can restart the signaling process through ligand dissociation.

Notably, introducing receptor synthesis and degradation can change both the directionality and magnitude of ligand-specific receptor activation and thus ligand discrimination. As seen in panel (A) of Fig. 4, the non-equilibrium discrimination ratio ε_N first decreases and then increases as a function of the dimensionless dissociation rate δ. This is because when preferential degradation β is sufficiently large, the slow-dissociating receptors are predominantly degraded leading to lower overall activity. In contrast, fast-dissociating receptors do not reach the ultimate receptor phosphorylation state due to frequent restarting of the signaling process. At high values of δ, the contribution of dissociation-driven signaling restart in the non-equilibrium flow increases, leading to traditional proofreading behavior. Notably, existence of slow and fast degraded active receptors is essential for the non-monotonic behavior; a signaling network with a single phosphorylated species ($N = 1$ in Fig. 3) does not exhibit non-monotonic discrimination. Finally, lengthening the multi-phosphorylation chain enhances discrimination in favor of the fast-dissociating ligand, albeit with diminishing returns.

In panel (B), we show the heat map of the discrimination rate ε_2 as a function of δ and β. The parameter β relates to cells' ability to preferentially degrade activated receptors which in turn can be controlled by changing expression of proteins involved in the degradation machinery. The dashed black line represents the contour ($\varepsilon_5 = 1$) that segregates signaling networks into those that prefer the slow-dissociating ligand (below) from those that prefer the fast-dissociating ligand (above). Notably, a high difference in dissociation rates ($\delta \gg 1$) allows for greater ligand discrimination in favor of either ligand as it sensitizes the discrimination ratio to changes in preferential degradation rate β. Importantly, the preferential degradation of activated receptors can be modulated by up or downregulating proteins comprising the ubiquitination machinery[33]. Therefore, depending on the context, cells may be able to choose their specificity in ligand encoding and downstream signaling.

Finally, the discrimination ratio depends non-monotonically on receptor phosphorylation rate ω. At very low ω, receptors bound to neither the slow-dissociating nor the fast-dissociating ligand reach the ultimate phosphorylation state associated with enhanced degradation. Consequently, the network prefers the slow-dissociating ligand, similar to the traditional proofreading scenario with no degradation. In contrast, as the phosphorylation rate increases, receptors bound to the slow-dissociating ligand are allowed to reach the ultimate phosphorylation state and are therefore degraded, leading to the network preferring the fast-dissociating ligand. As the phosphorylation rate increases sufficiently, the signaling network loses the ability to discriminate between the ligands as receptors bound to either of the ligands reaches the ultimate phosphorylation state and is degraded. In these calculations, the dissociation rate δ was fixed at $\delta = 10$.

Does the model with degradation also explain transient response observed in the EGFR pathway? It was observed that while the fast-dissociating ligands lead to a significantly higher *steady state* phosphorylation, the transient maximum phosphorylation levels were compa-

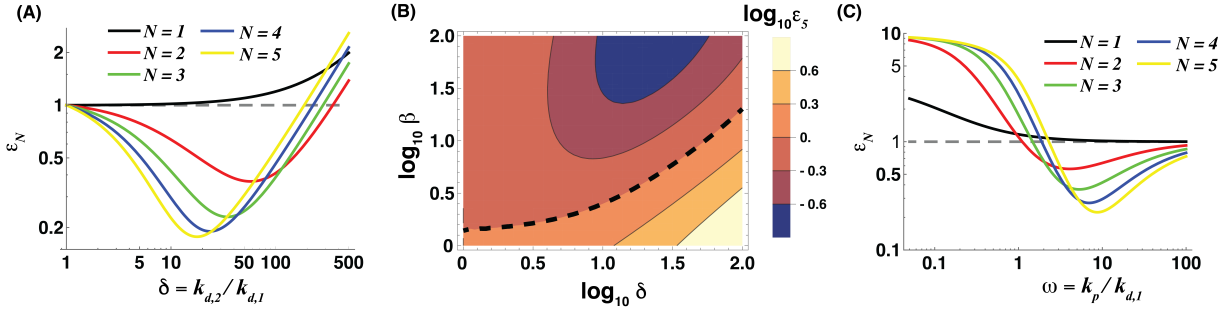

FIG. 4. **Kinetic proofreading in a model with receptor degradation**. (A) The non-equilibrium discrimination ratio ε_N plotted as a function of $\delta = k_{d,2}/k_{d,1}$for signaling networks with $N = 1 - 5$ steps of receptor phosphorylation. $\varepsilon_N < 1$ represent signaling networks that prefer weakly binding ligands . (B) Discrimination ratio ε_5 plotted as a function of $\log_{10}\beta$ and $\log_{10}\delta$ where $\beta = k^*_{\rm int}/k_{\rm int}$. The dashed black line shows the value of β that segregates networks that prefer the fast- and the slow-dissociating ligand. (C)ε_N plotted as a function of $\omega = k_p/k_{d,1}$. In panel (A), we have set $\beta = k^*_{\rm int}/k_{\rm int} = 50$ is the preferential degradation rate, $\omega = 10$, and $\gamma = k_{\rm int}/k_{d,1} = 0.05$ (dimensionless rate of inactive receptor internalization). In panel (B), we have set $\omega = 10$. In panel (C), we have set $\beta = 50$, $\delta = 10$ and $\gamma = 0.05$.

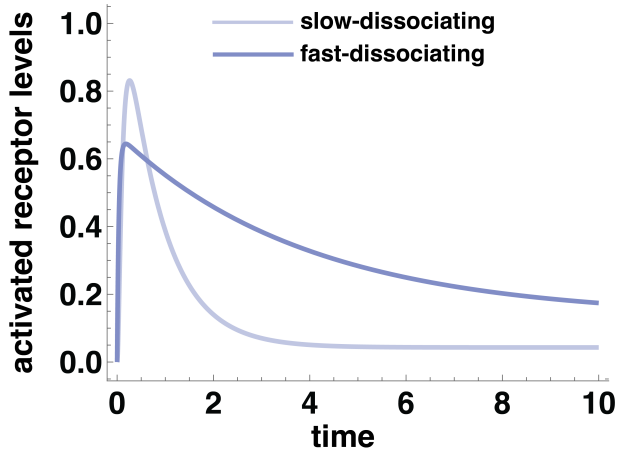

FIG. 5. **Transient dynamics of receptor activation for slow and fast-dissociating ligands**. We have used $\omega = 20$, $\delta = 10$, and $\gamma = k_{\rm int}/k_{d,1} = 0.05$, and $\beta = 50$. Ligand concentrations were set at $u_1 = 20$ and $u_2 = 2000$. The ligand concentrations are chosen based on dissociation constants estimated from Hu et al and concentrations taken from Freed et al.

rable for all ligands[29]. In Fig. 5, we show the transient phosphorylation dynamics following exposure to saturating concentrations of the two ligands respectively. In qualitative agreement with experimental observations, our model predicts that while the steady state phosphorylation activity is significantly higher for the fast-dissociating ligand, the transient phosphorylation activity is similar for the two ligands. This is because the transient activity depends largely on the phosphorylation rate ω and the steady state activity is governed by a competition between the ability of a ligand-bound receptor to reach the ultimate phosphorylation state (which depends on δ) and degradation of that state by the cellular machinery (which depends on the enhanced degradation rate β of activation receptors).

The discrimination in favor of the fast-dissociating ligand can also be realized with activity-induced desensitization. Here, an activated receptor becomes desensitized and unavailable for signaling for a brief *refractory* period before slowly recovering back to the sensitive state. The activity-induced desensitization motif is often observed in signaling networks associated with GPCRs[22] and ligand gated ion channels[23]. In Fig. 6, we show that similar to receptor degradation, activity-induced desensitization also allows the signaling network to favorably encode the fast-dissociating (low-affinity) ligand over the slow-dissociating (high-affinity) ligand tuning rate parameters unrelated to the ligand.

This discrimination in favor of the fast-dissociating ligand can be understood using a general *kinetic sorting* principle that allows signaling networks to modulate ligand discrimination in direction as well as magnitude. In our model, we discouraged the ligand-bound receptor to occupy the ultimate phosphorylation state by specifically targeting it for preferential degradation (or restarting). Depending on rate parameters, the signaling network *kinetically sorted* the non-equilibrium flux of receptors bound to the slow-dissociating (high-affinity) ligand towards degradation/desensitization. This preferential diversion of the non-equilibrium flux allowed the network to choose which ligand it discriminates against.

III. DISCUSSION

Ligand discrimination is an essential feature of many signaling networks that must encode an accurate representation of a complex and ever-changing environment[1,2]. Traditional kinetic proofreading mechanisms enhance the discrimination success between a 'correct' and an 'incorrect' ligand typically by exploiting differences in ligand dissociation rates. Notably, most kinetic proofreading

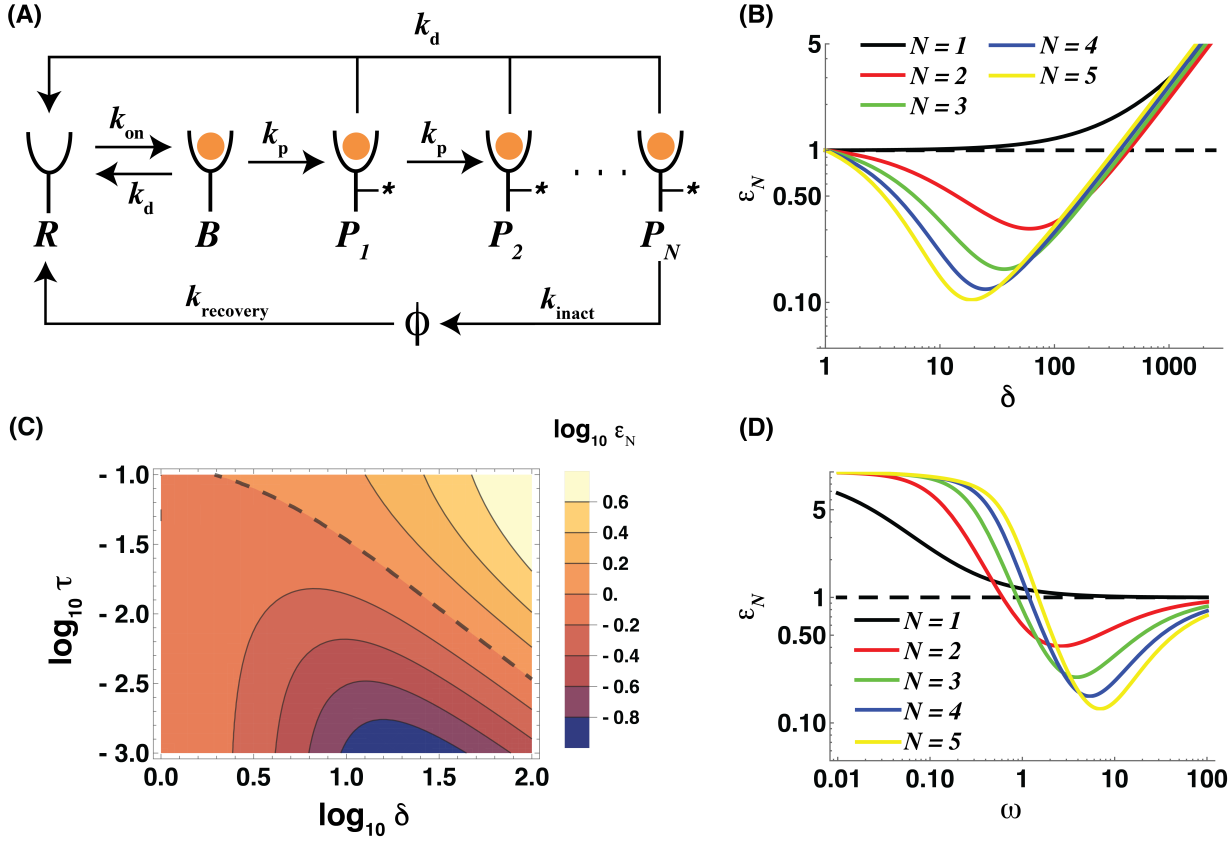

FIG. 6. **Kinetic proofreading in a model with activity-induced desensitization**. (A) The schematic of the model. B represents ligand-bound inactive receptor, and $P_m, m \in [1, N]$ are ligand-bound phosphorylated and signaling competent receptors. The state ϕ denotes inactivated receptors that cannot take part in signaling. (B) The non-equilibrium discrimination ratio ε_N plotted as a function of $\delta = k_{d,2}/k_{d,1}$for signaling networks with $N = 1 - 5$ steps of receptor phosphorylation. (C) Discrimination ratio ε_1 plotted as a function of $\log_{10}\tau$ and $\log_{10}\delta$ where $\tau = k_{\text{recovery}}/k_{d,1}$. The dashed black line shows τ that segregates networks that prefer the fast- and the slow-dissociating ligand. (D) The discrimination ratio ε_N plotted as a function of $\omega = k_p/k_{d,1}$. In panel (A), we have set $\tau = 0.001$, $\omega = 10$, and $\gamma = k_{\text{inact}}/k_{d,1} = 0.05$. In panel (B), we have set $\omega = 10$. In panel (C), we have set $\tau = 0.001$, $\delta = 10$ and $\gamma = 0.05$.

mechanisms operate only in one direction. They enhance the discrimination in favor of the correct ligand.

Similar to the current work, Murugan et al.[18] previously discussed an interesting *anti-proofreading* mechanism wherein biochemical networks can discriminate in favor of low-affinity ligands over the high-affinity ligands. In their work, a key requirement was that the non-equilibrium reaction network comprised of bidirectional reactions such that the log-ratio of equilibrium constants for the two ligands between the initial and the final state (in our case R and P_N) was independent of the path and only dependant on the free energy difference between the two ligands (in our case, the difference in dissociation rates δ). The authors delineated topological and kinetic requirements to guarantee that such a network discriminates in favor of low-affinity ligands over high-affinity ligands. However, our results represent a qualitatively distinct mechanism. Specifically, the cycles of receptor synthesis and degradation (and activity-induced inactivation) are truly unidirectional in that a degraded receptor/ligand complex will not *reconstitute* itself into a ligand-bound receptor. In other words, when a fully phosphorylated receptor P_N is 'returned' to the unbound receptor R through the degradation/desensitization cycle (Fig. 3 and panel (A) of Fig. 6), it does so in a manner that is independent of the ligand identity, providing a *kinetic wormhole* in the chemical state space between species P_N and R that is agnostic to the bound ligand. This is a crucial difference between the two models. We believe that these kinetic wormholes may allow extra freedom to signaling networks beyond what is possible by fully connected networks. We will further explore the role of such wormholes in a general context in future studies.

Here, we presented a simple model to explain how signaling networks may discriminate in favor of fast-dissociating (low-affinity) ligands over slow-dissociating (high-affinity) ligands at steady state. The model represents a novel *kinetic sorting* mechanism that combines kinetic proofreading with receptor degradation and activity-induced inactivation, common motifs in many

cellular signaling networks.

The biochemical processes included in our model can be broadly divided into those that rely on enzymes (receptor dephosphorylation and degradation) and those that depend on inherent biochemistry (ligand binding/unbinding and receptor autophosphorylation). Given that enzyme expression can vary substantially between tissue types[34] as well as among cells from any particular tissue[35], we expect that the rates associated with enzymatic reactions can be modulated through changes in protein abundance. In contrast, the rates that relate to the biochemical interactions between ligands and receptors are likely to be conserved. Therefore, cells are likely to have the freedom to tune the *kinetic sorting* mechanism in order to discriminate in favor of one ligand over another compared to the traditional proofreading mechanisms. Given the ubiquity of receptor degradation and activity induced inactivation, we believe that kinetic sorting is a broadly applicable mechanism of ligand discrimination.

IV. ACKNOWLEDGMENT

P. D. and A. G are funded by the NIGMS grant R35GM142547. R.R.M. is funded by a Sir Henry Wellcome Fellowship (220464/Z/20/Z).

V. SUPPLEMENTARY MATERIALS

All calculations below are performed using Mathematica. The notebooks are available at https://github.com/dixitpd/Kinetic_Sorting. In all cases, we assume that the steady state receptors levels in the absence of the ligand is equal to $R_0 = 1$.

A. Model equations

The system of equations governing the traditional proofreading network are given by:

$$\begin{aligned}
\frac{dR}{dt} &= k_{\text{delivery}} - k_{\text{on}}LR + k_d B + \sum_{n=1}^{N} k_d P_n - k_{\text{int}} R \\
\frac{dB}{dt} &= k_{\text{on}}LR - k_d B - k_p B + k_{dp} P_1 - k_{\text{int}} B \\
\frac{dP_n}{dt} &= k_p P_{n-1} - k_{dp} P_n - k_d P_n - k_{\text{int}} P_n \;\forall\; n \in [2, N-1] \\
\frac{dP_N}{dt} &= k_p P_{N-1} - k_{dp} P_N - k_d P_N - k^*_{\text{int}} P_N
\end{aligned} \tag{5}$$

In a model without degradation, we set $k_{\text{delivery}} = k_{\text{int}} = k^*_{\text{int}} = 0$. In the models solved in the main text, we assume that the dephosphorylation rate $k_{dp} = 0$. In Fig. S1, we show that inclusion of receptor dephosphorylation does not change the qualitative predictions from the model. These equations are solved at steady state

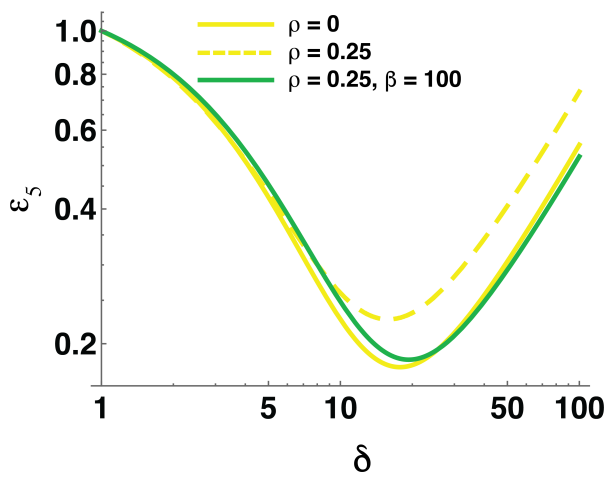

FIG. S1. **Effect of dephosphorylation on model behavior**. The non-equilibrium discrimination ratio ε_5 plotted as a function of $\delta = k_{d,2}/k_{d,1}$. We have introduced $\rho = k_{dp}/k_p$ is the dimensionless dephosphorylation rate. We have set $\beta = 50$, $\omega = 10$, and $\gamma = 0.05$.

(except for Fig. 5).

B. Modeling activity-induced desensitization

To model activity-induced desensitization, we modify the above equations as follows:

$$\begin{aligned}
\frac{dR}{dt} &= -k_{\text{on}}LR + k_dB + \sum_{n=1}^{N} k_dP_n + k_{\text{recovery}}\phi \\
\frac{dB}{dt} &= k_{\text{on}}LR - k_dB - k_pB + k_{dp}P_1 \\
\frac{dP_n}{dt} &= k_pP_{n-1} - k_{dp}P_n - k_dP_n \;\forall\; n \in [2, N-1] \\
\frac{dP_N}{dt} &= k_pP_{N-1} - k_{dp}P_N - k_dP_N - k^*_{\text{inact}}P_N \\
\frac{d\phi}{dt} &= k^*_{\text{inact}}P_N - k_{\text{recovery}}\phi
\end{aligned} \tag{6}$$

where ϕ is the desensitized state, k_{inact} is the desensitization rate of the ultimate activated receptor, and k_{recovery} is the recovery rate from the desensitized receptor.

C. Model with endosomal compartments

The system of equations governing the traditional proofreading network are given by:

$$\begin{aligned}
\frac{dR}{dt} &= k_{\text{delivery}} - k_{\text{on}}LR + k_dB + \sum_{n=1}^{N} k_dP_n - k_{\text{int}}R \\
&+ k_{\text{recycle}}R_i \\
\frac{dR_i}{dt} &= k_{\text{int}}R - k_{\text{recycle}}R_i - k_{\text{deg}}R_i \\
\frac{dB}{dt} &= k_{\text{on}}LR - k_dB - k_pB + k_{dp}P_1 - k_{\text{int}}B + k_{\text{recycle}}B_i \\
\frac{dB_i}{dt} &= k_{\text{int}}B - k_{\text{recycle}}B_i - k_{\text{deg}}B_i - k_pB_i + k_{dp}P_{1,i} \\
\frac{dP_n}{dt} &= k_pP_{n-1} - k_{dp}P_n - k_dP_n - k_{\text{int}}P_n \\
&+ k_{\text{recycle}}P_{n,i} \;\forall\; n \in [2, N-1] \\
\frac{dP_{n,i}}{dt} &= k_pP_{n-1,i} - k_{dp}P_{n,i} + k_{\text{int}}P_n - k_{\text{recycle}}P_{n,i} \\
&- k_{\text{deg}}P_{n,i} \;\forall\; n \in [2, N-1] \\
\frac{dP_N}{dt} &= k_pP_{N-1} - k_{dp}P_N - k_dP_N - k^*_{\text{int}}P_N \\
&+ k_{\text{recycle}}P^*_{N,i} \\
\frac{dP_{N,i}}{dt} &= k_pP_{N-1,i} - k_{dp}P_{N,i} + k^*_{\text{int}}P_N - k^*_{\text{recycle}}P^*_{N,i} \\
&- k_{\text{deg}}P_{N,i}
\end{aligned} \tag{7}$$

In a model without degradation, we set $k_{\text{delivery}} = k_{\text{int}} = k^*_{\text{int}} = 0$. In the models solved in the main text, we assume that the dephosphorylation rate $k_{dp} = 0$. Fig. S2 shows that inclusion of receptor dephosphorylation does not change the qualitative predictions from the model.

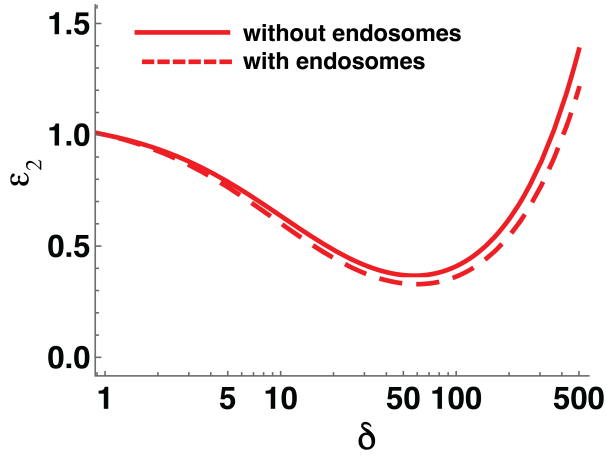

FIG. S2. **Effect of endosomal compartment on model behavior**. The non-equilibrium discrimination ratio ε_5 plotted as a function of $\delta = k_{d,2}/k_{d,1}$. We have introduced $\tau = k_{\text{recycle}}/k_{d,1} = 0.1$ as the dimensionless rate of endosomal recycling and $\theta = k_{\text{deg}}/k_{d,1} = 0.025$ as the dimensionless degradation rate. We have set $\beta = 50$, $\omega = 10$, and $\gamma = 0.05$.

VI. REFERENCES

[1] L. C. Cantley, T. Hunter, R. Sever, and J. W. Thorner, *Signal transduction: principles, pathways, and processes* (Cold Spring Harbor Laboratory Press Cold Spring Harbor, NY, USA:, 2014).
[2] R. R. Madsen and B. Vanhaesebroeck, Science Signaling **13**, eaay2940 (2020).
[3] R. R. Madsen *et al.*, bioRxiv , 2023 (2023).
[4] J. J. Hopfield, Proceedings of the National Academy of Sciences **71**, 4135 (1974).
[5] J. Ninio, Biochimie **57**, 587 (1975).
[6] K. Gulukota and P. G. Wolynes, Proceedings of the National Academy of Sciences **91**, 9292 (1994).
[7] J. Yan, M. O. Magnasco, and J. F. Marko, Nature **401**, 932 (1999).
[8] J. J. Hopfield, Proceedings of the National Academy of Sciences **77**, 5248 (1980).
[9] P. Hilleren and R. PARKER, Rna **5**, 711 (1999).
[10] T. W. McKeithan, Proceedings of the national academy of sciences **92**, 5042 (1995).
[11] W. Y. Huang *et al.*, Science **363**, 1098 (2019).
[12] R. Mukherjee, A. Sengar, J. Cabello-García, and T. E. Ouldridge, Journal of the American Chemical Society **146**, 18916 (2024).
[13] A. Murugan, D. A. Huse, and S. Leibler, Proceedings of the National Academy of Sciences **109**, 12034 (2012).
[14] R. Rao and L. Peliti, Journal of Statistical Mechanics: Theory and Experiment **2015**, P06001 (2015).
[15] H. Boeger, Annual Review of Biochemistry **91**, 423 (2022).
[16] R. Ravasio *et al.*, arXiv preprint arXiv:2405.10911 (2024).
[17] V. Galstyan, K. Husain, F. Xiao, A. Murugan, and R. Phillips, Elife **9**, e60415 (2020).
[18] A. Murugan, D. A. Huse, and S. Leibler, Physical Review X **4**, 021016 (2014).
[19] B. Singh, G. Carpenter, and R. J. Coffey, F1000Research **5** (2016).
[20] A. Sorkin and L. K. Goh, Experimental cell research **315**, 683 (2009).
[21] R. Irannejad and M. Von Zastrow, Current opinion in cell biology **27**, 109 (2014).

[22]E. Kelly, C. P. Bailey, and G. Henderson, British journal of pharmacology **153**, S379 (2008).
[23]M. Gielen and P.-J. Corringer, The Journal of Physiology **596**, 1873 (2018).
[24]T. Shi *et al.*, Science Signaling **9**, rs6 (2016).
[25]E. Lyashenko *et al.*, Elife **9**, e50342 (2020).
[26]R. Milo, P. Jorgensen, U. Moran, G. Weber, and M. Springer, Nucleic acids research **38**, D750 (2010).
[27]L. B. Kleiman, T. Maiwald, H. Conzelmann, D. A. Lauffenburger, and P. K. Sorger, Molecular cell **43**, 723 (2011).
[28]S. Feng *et al.*, bioRxiv (2023).
[29]D. M. Freed *et al.*, Cell **171**, 683 (2017).
[30]R. R. Madsen and A. Toker, Journal of Biological Chemistry **299** (2023).
[31]H. S. Wiley, The EGF Receptor Family , 81 (2003).
[32]C. Hu *et al.*, Nature **602**, 518 (2022).
[33]B. Mohapatra *et al.*, Biochimica Et Biophysica Acta (BBA)-Molecular Cell Research **1833**, 122 (2013).
[34]J. Lonsdale *et al.*, Nature genetics **45**, 580 (2013).
[35]M. Niepel, S. L. Spencer, and P. K. Sorger, Current opinion in chemical biology **13**, 556 (2009).

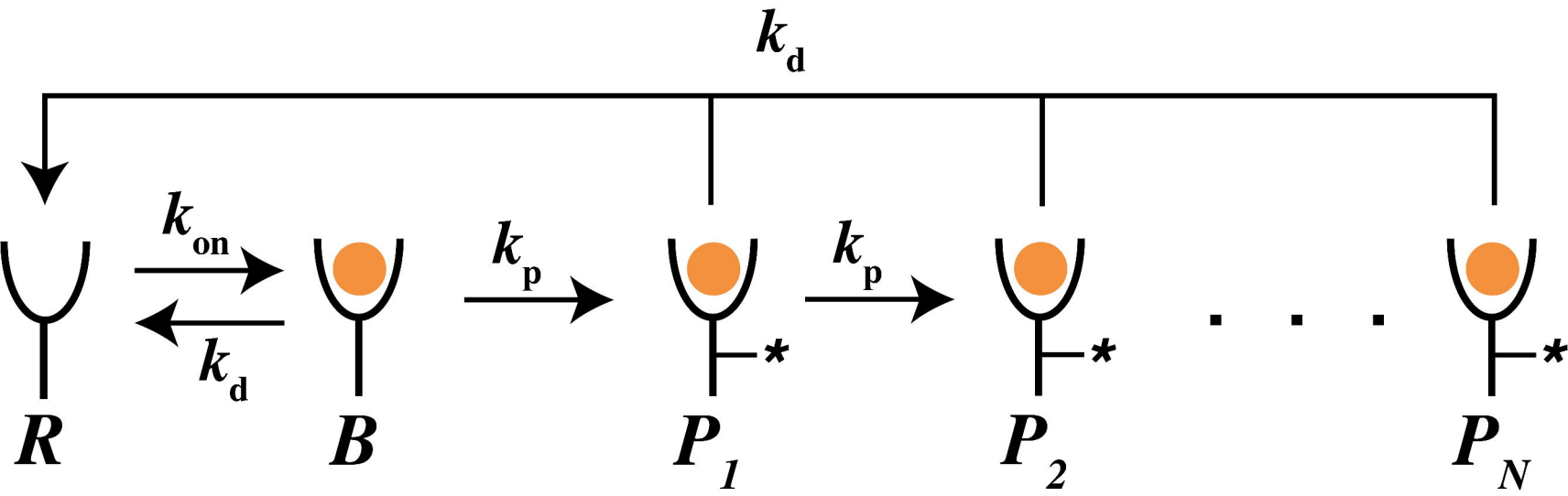
k_d
k_{on}
k_d
k_p
k_p
*
*
*
R
B
P_1
P_2
P_N

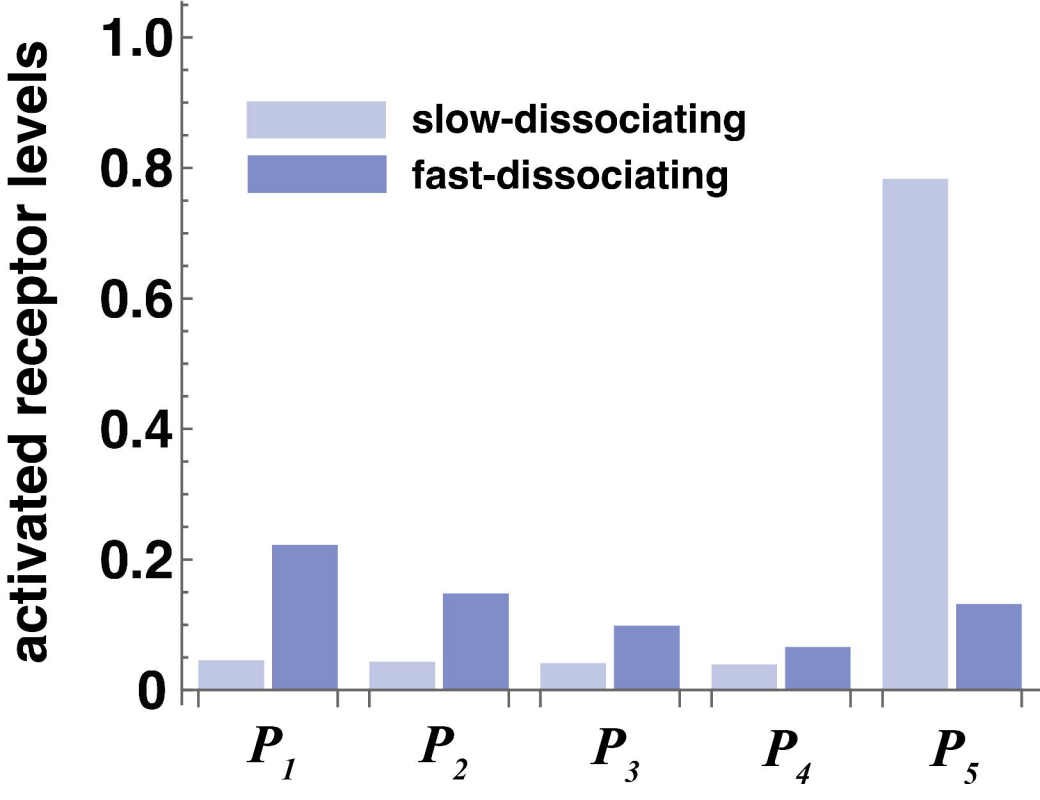
activated receptor levels
1.0
0.8
0.6
0.4
0.2
0
slow-dissociating
fast-dissociating
P_1
P_2
P_3
P_4
P_5

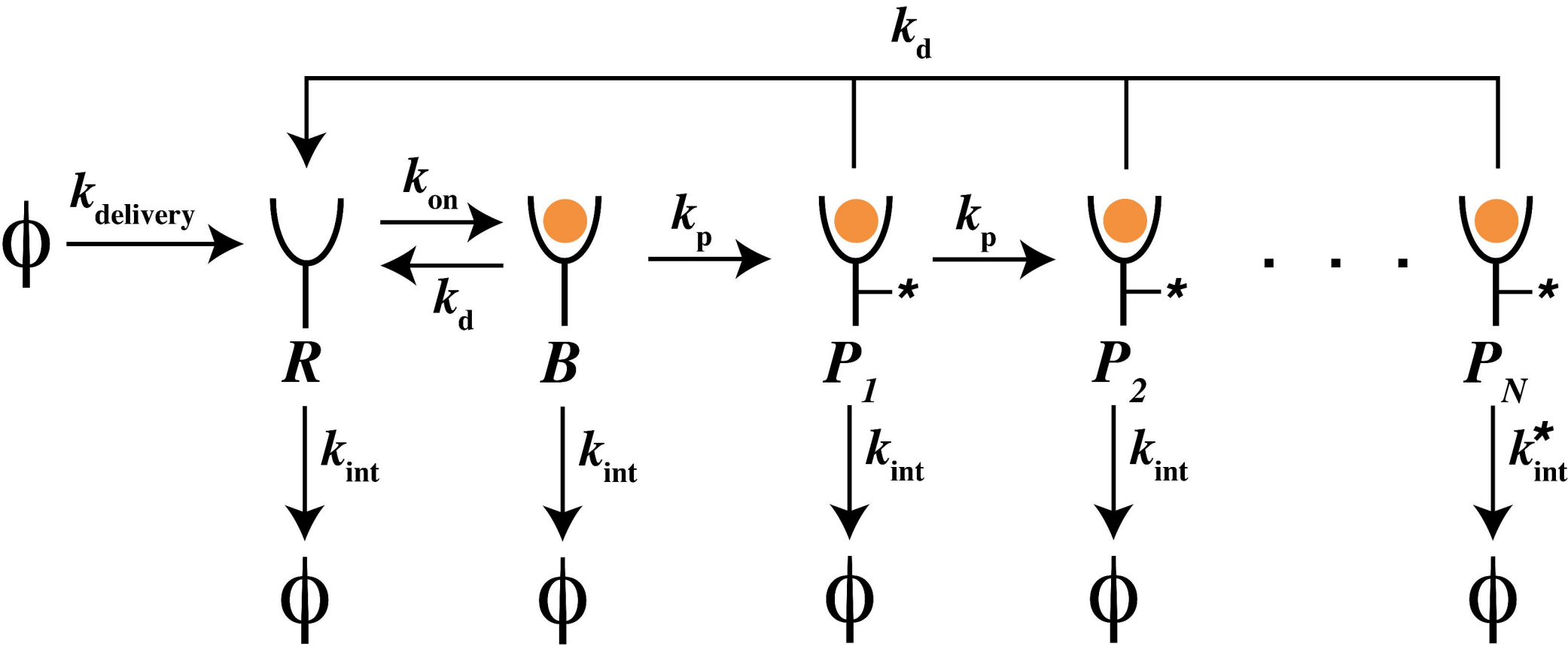
k_d
ϕ
$k_{delivery}$
k_{on}
k_d
k_p
k_p
R
B
P_1
P_2
P_N
k_{int}
k_{int}
k_{int}
k_{int}
k^*_{int}
ϕ
ϕ
ϕ
ϕ
ϕ

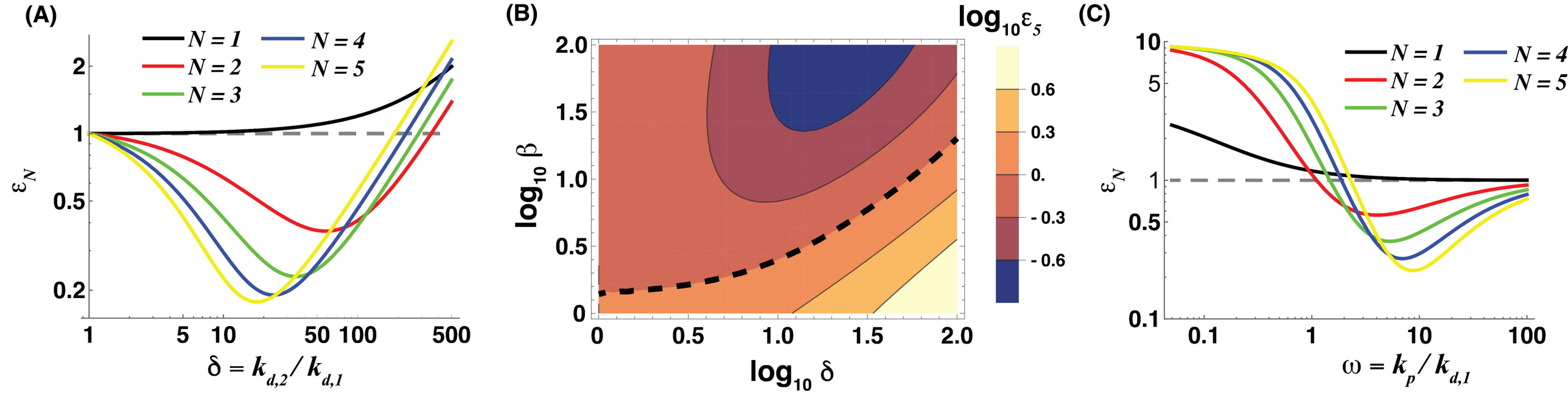
(A)
N = 1
N = 2
N = 3
N = 4
N = 5
ε_N
2
1
0.5
0.2
1
5
10
50
100
500
$\delta = k_{d,2}/k_{d,1}$
(B)
$\log_{10}\varepsilon_5$
0.6
0.3
0.
- 0.3
- 0.6
$\log_{10}\beta$
2.0
1.5
1.0
0.5
0
0
0.5
1.0
1.5
2.0
$\log_{10}\delta$
(C)
N = 1
N = 2
N = 3
N = 4
N = 5
ε_N
10
5
1
0.5
0.1
0.1
1
10
100
$\omega = k_p/k_{d,1}$

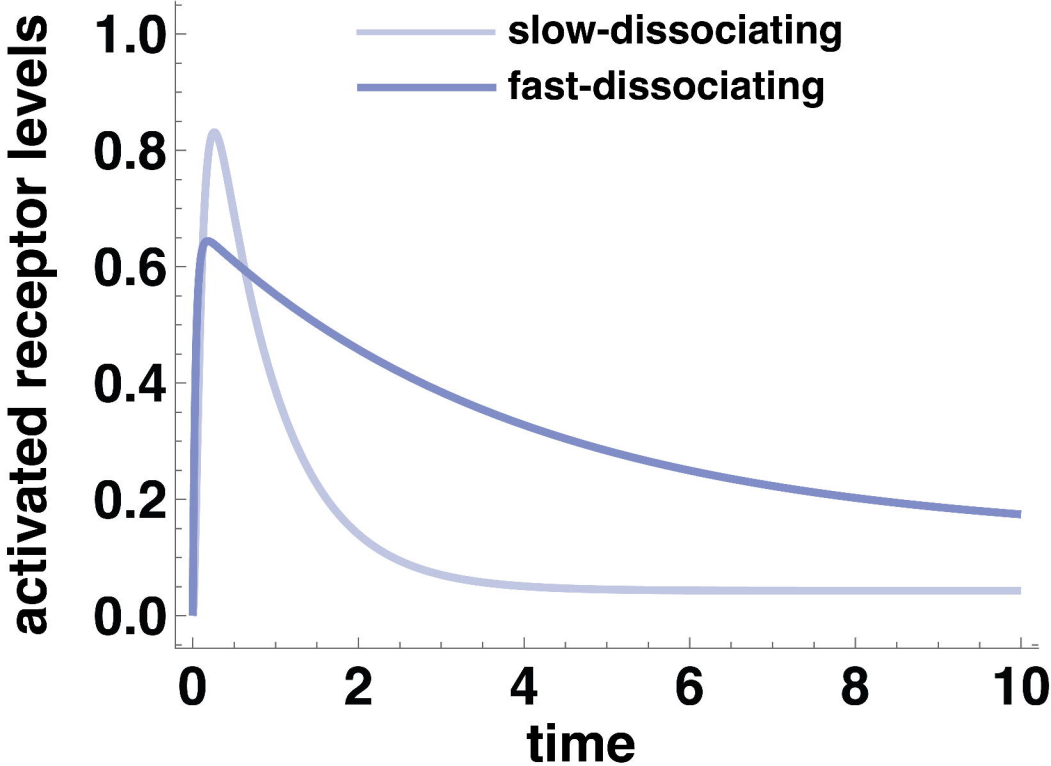
slow-dissociating
fast-dissociating
activated receptor levels
1.0
0.8
0.6
0.4
0.2
0.0
0
2
4
6
8
10
time

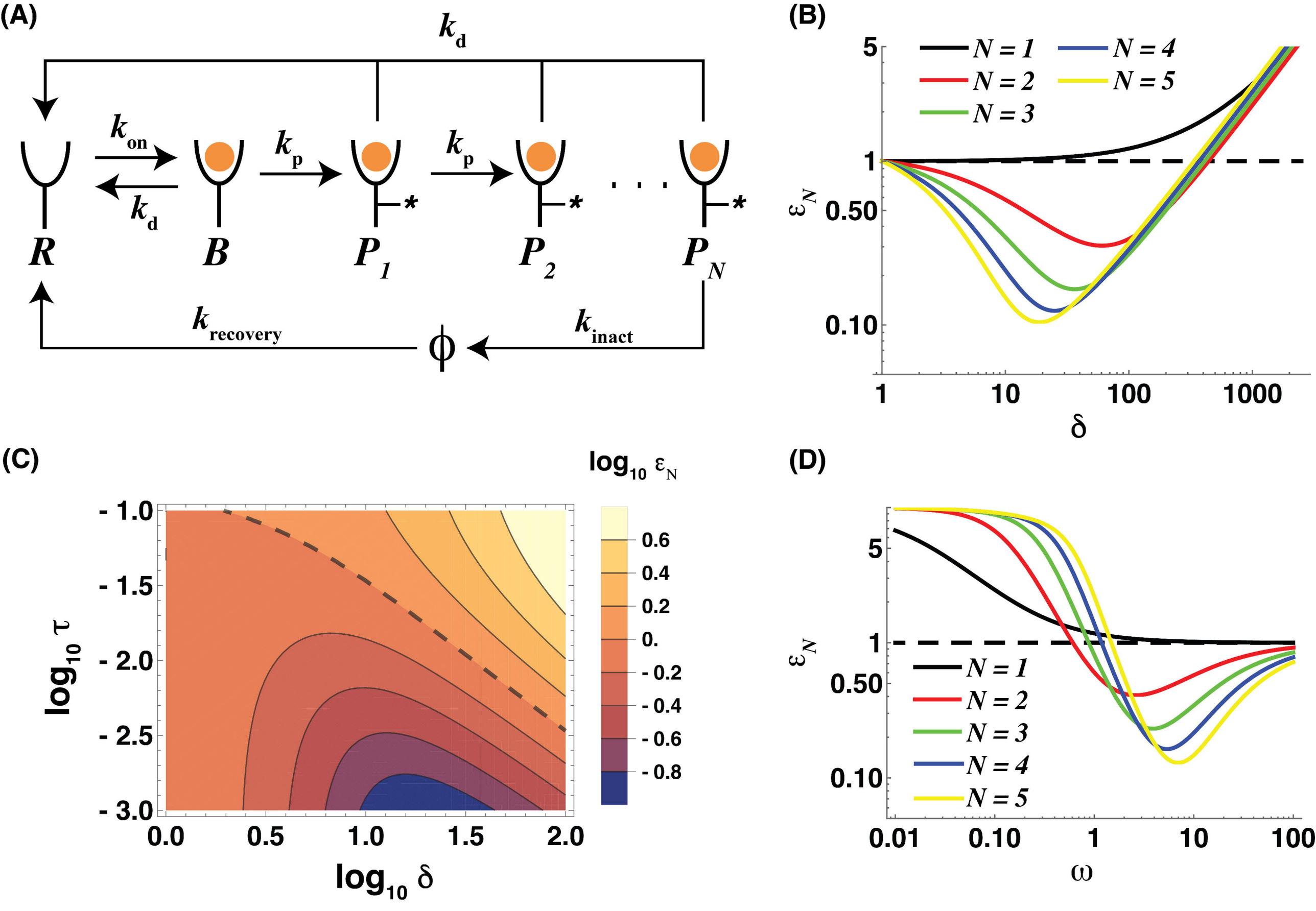
(A)
k_d
k_{on}
k_d
k_p
k_p
R
B
P_1
P_2
P_N
$k_{recovery}$
k_{inact}
ϕ
(B)
N = 1
N = 2
N = 3
N = 4
N = 5
ε_N
δ
(C)
$\log_{10} \varepsilon_N$
$\log_{10} \tau$
$\log_{10} \delta$
(D)
ε_N
ω

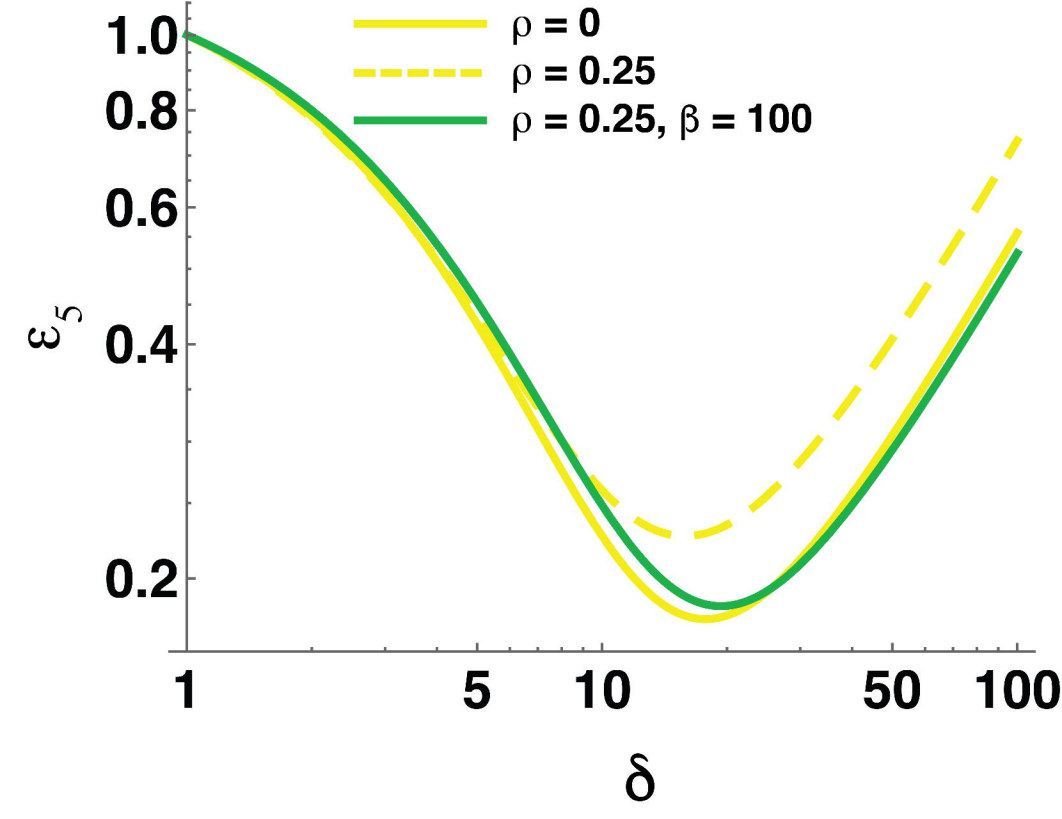
ρ = 0
ρ = 0.25
ρ = 0.25, β = 100
1.0
0.8
0.6
0.4
0.2
ε5
1
5
10
50
100
δ

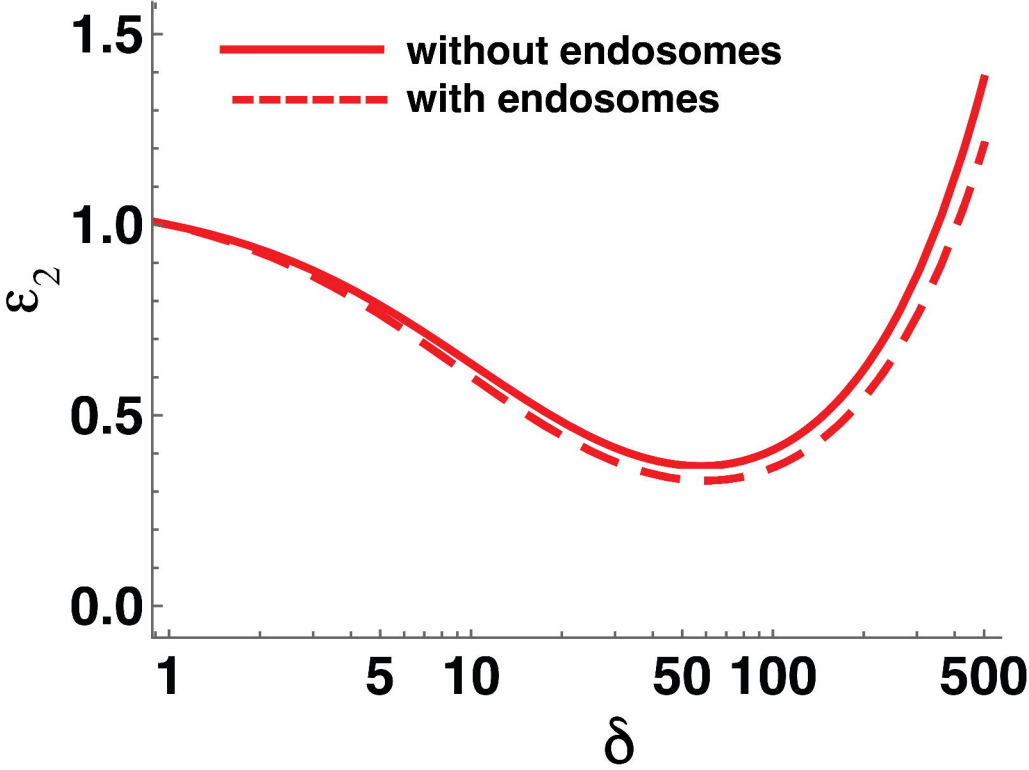
without endosomes
with endosomes
1.5
1.0
0.5
0.0
ε_2
1
5
10
50
100
500
δ